Au_{60}^-: The Smallest Gold Cluster with the High-Symmetry Icosahedral Core Au_{13}

Seema Pande,[1] Xingao Gong,[2]
Lai-Sheng Wang,[3] and Xiao Cheng Zeng[1]

1 Department of Chemistry, University of Nebraska–Lincoln, Lincoln, Nebraska 68588, United States
2 Department of Physics, Key Laboratory for Computational Physical Science (Ministry of Education), Fudan University, Shanghai 200433, China
3 Department of Chemistry, Brown University, Providence, Rhode Island 02912, United States

Corresponding authors — xggong@fudan.edu.cn ; Lai-Sheng_Wang@Brown.edu ; xzeng1@unl.edu

ORCID
Lai-Sheng Wang: 0000-0003-1816-5738
Xiao Cheng Zeng: 0000-0003-4672-8585

Abstract:
Among coinage metal nanoclusters with 55 atoms, only Ag_{55}^- and Cu_{55}^- are the geometric magic-number clusters, as both exhibit icosahedral symmetry. Au_{55}^-, however, exhibits much lower symmetry due largely to the strong relativistic bonding effect. In this study, we collect a much larger population (>10,000 isomers) of low-energy isomers of Au_{55}^- to Au_{60}^- by using the combined density-functional theory and basin-hopping global optimization method. We also include the spin−orbit effect in the density-functional theory computation to achieve simulated photoelectron spectra in quantitative fashion. Remarkably, we uncover that the Au_{13} core with the highest icosahedral (I_h) symmetry emerges at the size of Au_{60}^-. Stability analysis suggests that Au_{57}^- with 58 valence electrons, an electronic magic number, is the relatively more stable cluster in the size range considered. Overall, in this size range we reveal a compromise between the trend toward having a perfect icosahedral 13-atom core and the strong relativistic bonding effect.

Published in *The Journal of Physical Chemistry Letters* 10 (2019), pp 1820-1827.
DOI: 10.1021/acs.jpclett.9b00446

Submitted February 17, 2019; accepted March 29, 2019; published March 29, 2019.
Supporting Information follows the References.

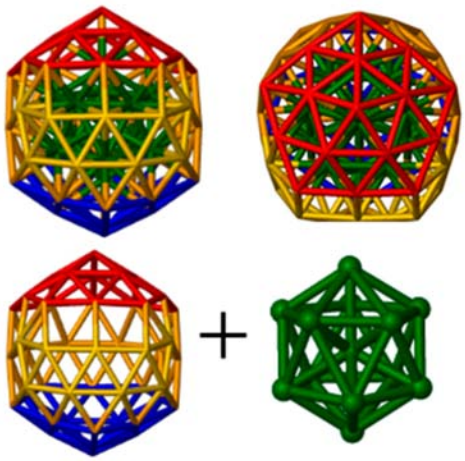

Clusters that possess the icosahedral symmetry belong to a class of geometric magic-number clusters.[1,2] A well-known hollow-cage cluster with the perfect icosahedral symmetry is the buckminsterfullerene C_{60}.[3] Compact metal clusters with either 13 or 55 atoms also tend to be good candidates to exhibit the icosahedral symmetry as both sizes can be found in the Mackay icosahedral series.[1,2] For the 13-atom transition metal clusters, Piotrowski et al. showed that icosahedral-like forms are favorable only in early 3d, 4d, and 5d series.[4] For coinage metal elements, first-principles computations have shown that the icosahedral structure of M_{13} (M = Cu, Ag, Au) is unfavorable, due to their relatively high energy.[5,7] Indeed, for Ag and Cu, the smallest icosahedral clusters are at the size of 55 atoms. Also, both Ag_{55}^- and Cu_{55}^- can be viewed as a core−shell cluster with the 13-atom icosahedral core and 42-atom icosahedral outer shell.[8−12] Au_{55}^-, however, exhibits much lower symmetry due largely to the strong relativistic bonding effect.[8,12] For neutral Au_{55}, Garzón et al. perhaps were the first to predict that the high-symmetry icosahedral structure and low-symmetry structures are degenerate in energy,[13] while Huang et al. showed convincingly from a joint experimental/theoretical study that Au_{55}^- is a low-symmetry structure.[14] Naturally, one can ask whether a compact core−shell gold cluster can entail a 13-atom high-symmetry icosahedral core, and at what size if such a high-symmetry core could arise.

Structural evolution of gold clusters have been extensively studied over the past two decades due in part to gold clusters' remarkable catalytic activities. Particular attention, for example, has been

placed on the size- and support-dependent CO oxidation,[15,18] and the structure−activity relationships.[19,20] Among midsized gold clusters with 20−60 atoms, only a few exhibit highly symmetric structures.[21,22] The pyramidal Au_{20}^- exhibits the perfect tetrahedral symmetry due largely to electronic shell closing of the neutral isomer so that the additional electron does not break the high symmetry.[23] Metal clusters with the total number of valence electrons of 2, 8, 18, 20, 34, 40, or 58 belong to electronic-shell closure, a notion first introduced for understanding electronic magic numbers in alkali metal clusters.[24] Notably, our previous joint experimental and theoretical studies have shown that Au_{33}^- to Au_{42}^- are all core−shell clusters with a highly symmetric four-atom tetrahedral core.[25−27] Au_{46}^- and Au_{47}^- are also core−shell clusters with a pyramidal fragment stacked with another truncated pyramid.[27] In this study, our focus is placed on the size range of Au_n^- (n = 55−60). We use the unbiased basin-hopping global optimization method combined with density-functional theory (DFT) optimization[28,30] to obtain a much larger population of low-energy isomers. Most importantly, we consider the spin−orbit (SO) effect in the density-functional theory computation of the simulated anion photoelectron (PE) spectra of all low-lying isomers for each size of gold clusters. Our previous studies have shown that the inclusion of SO effects can give rise to nearly quantitative match between the simulated and measured PE spectra for gold clusters.[25−27,31−36]

The gradient-corrected Perdew−Burke−Ernzerhof (PBE) exchange−correlation functional[37] and the double-numerical polarized (DNP) basis set with effective core potential (ECP), as implemented in the DMol 4.0 program,[38,39] is employed for the geometry optimization of about 1200−2000 isomers obtained from the unbiased basin-hopping search for each size of anionic gold clusters, with convergence of 1×10^{-5} H. Among the top 100 low-energy isomers, those with the energy gap between the first and second vertical detachment energy (VDE) being close to the measured energy gap between the first and second VDE are selected for reoptimization using a higher-level theory of PBE0/TZP(ECP) (triple-ζ polarization) with inclusion of the relativistic effects under zeroth-order regular approximation (ZORA), as implemented in the ADF2013 software package.[40−42] The simulated PE spectra of these ADF-optimized candidate isomers (about 15 for each size of clusters) are then obtained by using the hybrid PBE0[43] functional with inclusion of the spin−orbit (SO) effects (hereafter referred

as SO-PBE0 method), as implemented in the NWCHEM 6.6[44] software package. For relatively smaller clusters, n = 55−58, we use the CRENBL(ECP)[45] basis set, while for the larger two clusters, n = 59, 60, we use the dhf-SV(P) (ECP)[46] basis set, as CRENBL(ECP) becomes increasingly expensive for larger sized clusters. Lastly, the simulated PE spectra are used to compare with the measured PE spectra, as done in previous studies.[25−27,31−36] The isomers that give rise to the best match with the measured PE spectra are identified as the most stable isomers in the experimental cluster beam.

Isomer Assignment

There is often more than one low-lying candidate isomer for midsized gold clusters. We have identified one isomer of Au_{55}^- and two each for Au_n^- (n = 56−60) that are the most likely present in the cluster beam. In **Table 1** we present the experimental first VDE and theoretical first VDE's of all assigned isomers. As anticipated from experiences of previous studies, the SO-PBE0 method tends to give simulated spectra with a systematic red shift in the computed binding energies. Thus, the theoretical VDE's are smaller in value compared to the experimental ones. In Table 1, we also compare the measured energy gap (X−A

Table 1. Experimental First VDE and X−A Gap of Au_n^- (n = 55-60)* and Theoretical First VDE, X−A Gap, Relative Energies [Based on SO-PBE0/CRENBL(ECP) for n = 55−58 and SO-PBE0/dhf-SV(P)(ECP) for n = 59−60], RMSD, and Number of Core Atoms of the Assigned Core-Shell Isomers (All Energy Values in eV).

	Experimental*		Theoretical					
n in Au_n^-	First VDE	X−A gap	Isomer	No. of core atoms	First VDE	X−A gap	ΔE	RMSD
55	4.33	0.07	I	10	4.12	0.10	0	0.049
56	4.15	0.23	I	10	3.91	0.21	0	0.030
			II	9	3.89	0.29	0.08	0.070
57	4.31	0.06	I	12	4.17	0.09	0.01	0.069
			II	12	4.20	0.13	0	0.106
58	3.79	0.65	I	12	3.61	0.58	0	0.078
			II	12	3.62	0.61	0.02	0.074
59	3.88	0.62	I	12	3.63	0.63	0	0.026
			II	12	3.57	0.68	0.04	0.081
60	3.68	0.21	I	13	3.36	0.19	0	0.089
			II	13	3.37	0.21	0.05	0.119

* From ref 14.

gap) between the first and second VDE, which corresponds to the energy difference between the first two highest peaks (X and A peaks), with the computed energy gap between the first and second major peaks in the simulated spectrum. Notably, the computed energy gap for assigned major isomer I is very close to the measured X−A gap in all cases. For all clusters considered, the difference in the X−A gap is within 0.03 eV except for Au_{58}^-. The latter, however, has a broad first peak (X) in the experimental spectrum (see Figure 1d). As shown in Table 1, the low-lying isomers are relatively degenerate in energy based on the SO-PBE0 computation (ΔE in Table 1). For gold anion clusters, the M06 functional is known to be a reliable functional for assessing relative stabilities among gold isomers with very close energies.[47] Our previous studies show that the SO-PBE0/CRENBL (ECP) level of theory can give nearly the same trend in term of relative energies among gold isomers as that given by M06/cc-pVDZ-pp (ECP).[27] The electronic properties of other candidate isomers are given in **Tables S1 – S6**.

Parts a−f of **Figure 1** display the experimental spectra (red),[14] where the peaks labeled X, A, B, ... represent the first, second, and third, ... VDE, respectively. The simulated spectra (black) of assigned isomers (I for major and II for minor isomer) are also presented in Figure 1. It can be seen that the simulated spectra of the assigned isomers match the experimental spectra nearly quantitatively for the first ten major peaks or so. We therefore label the corresponding peaks as X, A, B, etc. in the simulated spectra for ease of comparison. Since the relative energies of the low-lying isomers are extremely close, the spectral peak-for-peak match is the most important indicator for identifying the major and minor isomers. Some low-energy isomers, despite being close in energy with the major isomer, can still be ruled out due to their simulated spectra are not in good agreement with the measured spectra (**Figures S1 – S6**).

For Au_{55}^-, we assign only a single isomer because not only this isomer can already produce all spectral features (X, A−I peaks in Figure 1a) but also none of the other low-lying isomers can yield a simulated spectrum in quantitative fashion (see Figure S1). To quantitatively measure the agreement between the simulated spectrum of the major isomer and the measured spectrum, we calculate the root-mean-square deviation (RMSD) for the major labeled peaks between experiment and simulation, as done previously.[27,31] In short, we align the first peak (X peak) of the theoretical spectra with experimental

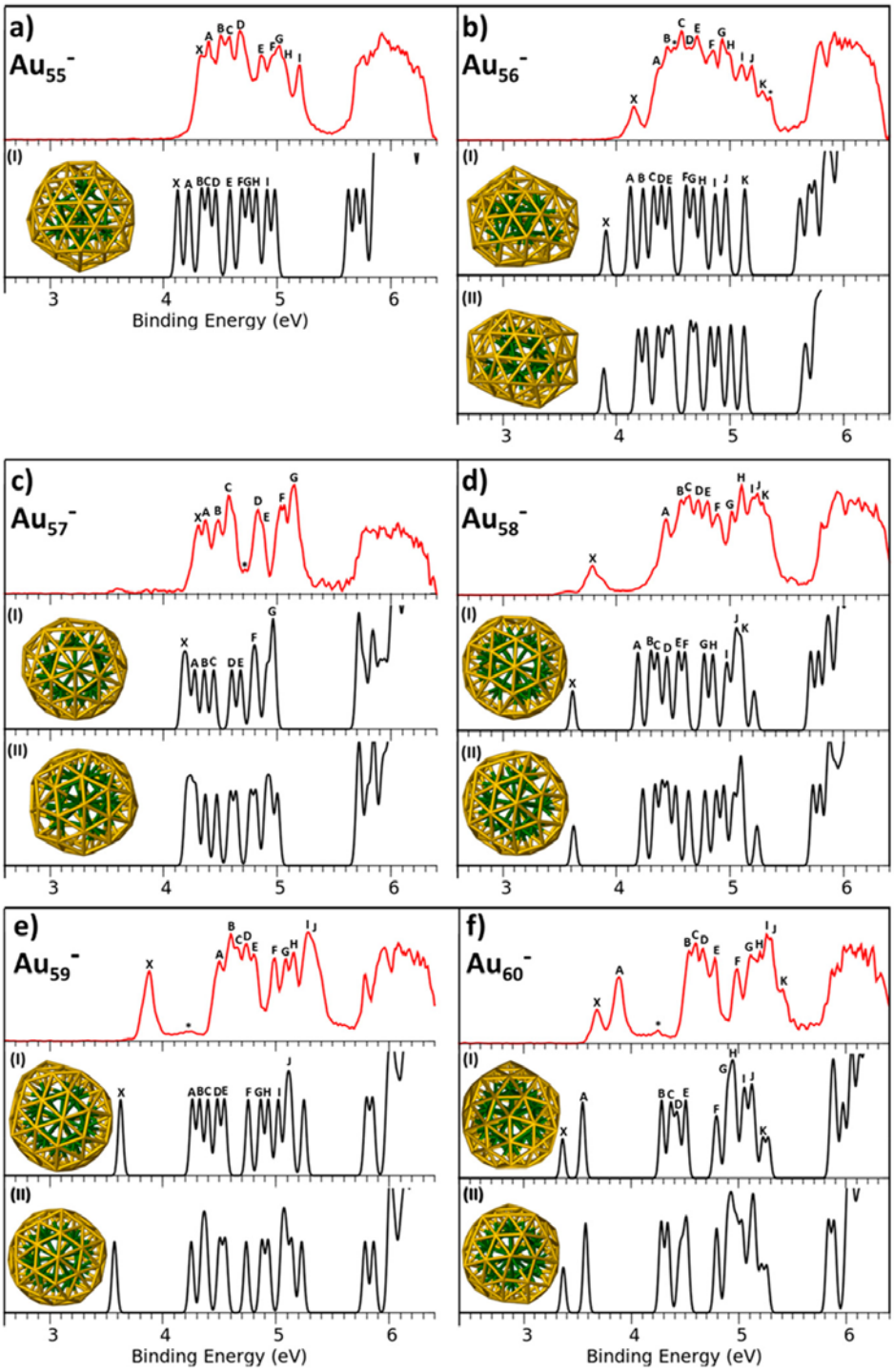

Figure 1. (a)−(f) Comparison of experimental photoelectron spectra of Au_n^- (n = 55−60) (red) and with simulated spectra of assigned isomers (black). The * in the experimental photoelectron spectra represent very weak features likely contributed by minor isomers. The core atoms are highlighted in green, while the outer shell atoms are in yellow. The RMSD values shown in Table 1 are computed on the basis of all labeled peaks (A, B, ...).

first VDE and then calculate the deviation of corresponding peaks labeled (A, B, C, ...) in Figure 1. The RMSD values are presented in Table 1, which provide further credence that the assigned isomers are likely the best candidate. For Au_{56}^-, the simulated spectrum of major isomer I gives rise to all the major peaks (X, A−K; RMSD = 0.03 eV), while the minor isomer II may also be present in the cluster beam, as it may contribute to the major and minor peaks in the spectrum (Figure 1b). Similarly, for Au_{57}^-, we assign a major isomer I, as it can give all major peaks (X, A−G; RMSD = 0.069 eV), and a minor isomer II, which seems to contribute some major and minor features of the measured spectrum. Lastly, for Au_n^- (n = 58, 59, 60), we assign two isomers for each size. The major isomer I not only is the lowest-energy isomer based on the SO-PBE0 computation but also gives all the major spectral features of the experimental spectra (X, A− K n = 58; X, A−J n = 59; and X, A−K, for n = 60; RMSD values in Table 1). The minor isomer II in all three cases may also contribute to the spectral features with reasonably small RMSD values. Hence, isomer II is not ruled out. Overall, the isomers newly identified in this study are notably lower in energy than previously reported isomers[14] (see Tables S1−S6). With the inclusion of the SO effects in our calculations, we observe splitting of peaks in simulated spectra of these isomers. Simulated spectra based on SO-PBE0 computation for previously reported isomers[14] are also given in Figures S1−S6.

Structural Evolution from Au_{55}^- to Au_{59}^-

The structural evolution in the size range of n = 55−59 is analyzed in more detail, on the basis of all newly assigned major isomers (Figure 1). As reported previously,[14] the most stable clusters in this size range exhibit the core−shell structures (**Figure 2**). Here, the core of Au_{55}^- and Au_{56}^- exhibits a 10-atom structure with a central atom although isomer II of Au_{56}^- exhibits a nine-atom core. The arrangement of these core atoms appears like an icosahedron missing three apex atoms. Both major and minor isomers of Au_{57}^-, Au_{58}^-, and Au_{59}^- exhibit a 12-atom icosahedral core missing only one apex atom[14] (insets in Figure 2). Previously, the cavity region due to the missing apex atom was referred as a small bubble.[14,48] The fact that the 11-atom core is not shown in the structural evolution of the gold clusters in the size range considered suggests that the 11-atom icosahedron with two missing apex atoms appears to be energetically unfavorable as the inner core.

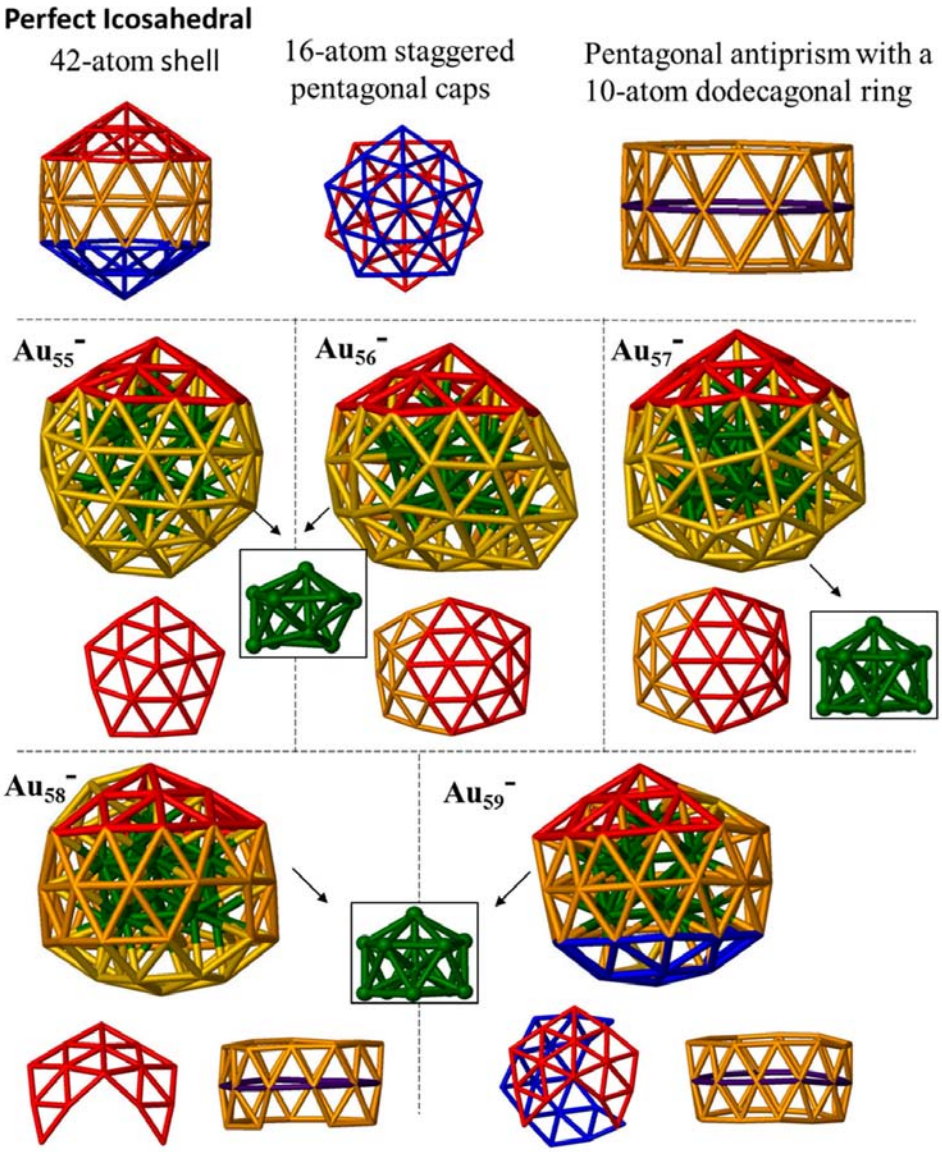

Figure 2. Top panel: perfect icosahedron shell of 42 atoms with two pentagonal caps (red and blue) and a pentagon antiprism containing a 10-atom dodecagonal ring (purple). Middle and bottom panels: same color coding used to compare the assigned major structures of Au^- (n = 55−59). Red and blue highlight fragments of pentagon cap, while the purple color highlights the 11-atom ring. Insets in green display the core structure.

Interestingly, the outer shells of the major isomers also exhibit some resemblances to an icosahedron. In a perfect 55-atom Mackay icosahedron, the core consists of 13-atoms, while the outer shell has 42 atoms (see Figure 2). In the outer shell, 32 atoms form two opposing pentagonal caps in staggered conformation while the remaining 10 atoms form a dodecagonal ring structure in the pentagonal

antiprism section of icosahedron. (Figure 2). Clearly, the isomer I of Au_{55}^- is a low-symmetry structure. But its outer shell exhibits a 16-atom pentagonal cap (red), highly resembling the cap of an icosahedron (Figure 2). Similar pentagonal cap and antiprism fragments can be also seen in the outer shell of both Au_{56}^- and Au_{57}^-. In Au_{58}^- and Au_{59}^-, an 11-atom ring structure can be observed, resembling the dodecagonal ring of a perfect Mackay icosahedron. The middle section consisting of 32- and 33-atoms, respectively, resembles the distorted pentagonal antiprism structure. Au_{58}^- also exhibits a fragment of pentagon cap and Au_{59}^- exhibits two fragments of pentagon caps in staggered confirmation. Hence, from Au_{55}^- to Au_{59}^-, increasing the number of fragments that resemble those of a perfect Mackay icosahedron can be observed. Similar color-coded structures of minor isomers are presented in **Figure S7**.

There are some differences between the isomers assigned in this study and the isomers assigned in the previous study.[14] Specifically, in this study, the 12-atom icosahedral core with the missing apex atom emerges at Au_{57}^- and is also present in both Au_{58}^- and Au_{59}^-. In the previous study,[14] it was found that filling the surface holes of the distorted Au_{55}^- can yield a near-spherical core−shell Au_{58}^- structure with the 12-atom icosahedral core with the missing apex atom while the outer shell exhibits six square-defect sites.[14] It was also found that the outer shell of Au_{59}^- can be constructed by adding an extra atom to a defect site in the outer shell of Au_{58}^-, resulting in one less square defect site (see **Figure 3**, where the isomers reported in reference 14 are labeled as ref-14). Although in both studies, Au_{58}^- and Au_{59}^- are predicted to possess the same 12-atom core, the outer shells exhibit some dissimilarities (Figure 3). The isomer I of Au_{58}^- exhibits a pentagonal defect and three square defects, while isomer II exhibits a pentagonal defect and four square defects (two of which are in the backside). Isomer I and isomer II of Au_{59}^- exhibit four and three square defects, respectively, and both isomers appear to be more spherical than the isomer ref-14. To characterize the delicate structural difference among these predicted isomers, we plot the relative-distance distribution, with respect to the center of mass, of all atoms (Figure S8). In general, the isomers predicted in this study appear to be more compact than the isomers predicted from ref 14. Note also that the predicted most stable isomer of Au_{58} in ref 14 was initially obtained from first-principles molecular dynamics simulation of neutral Au_{58}.

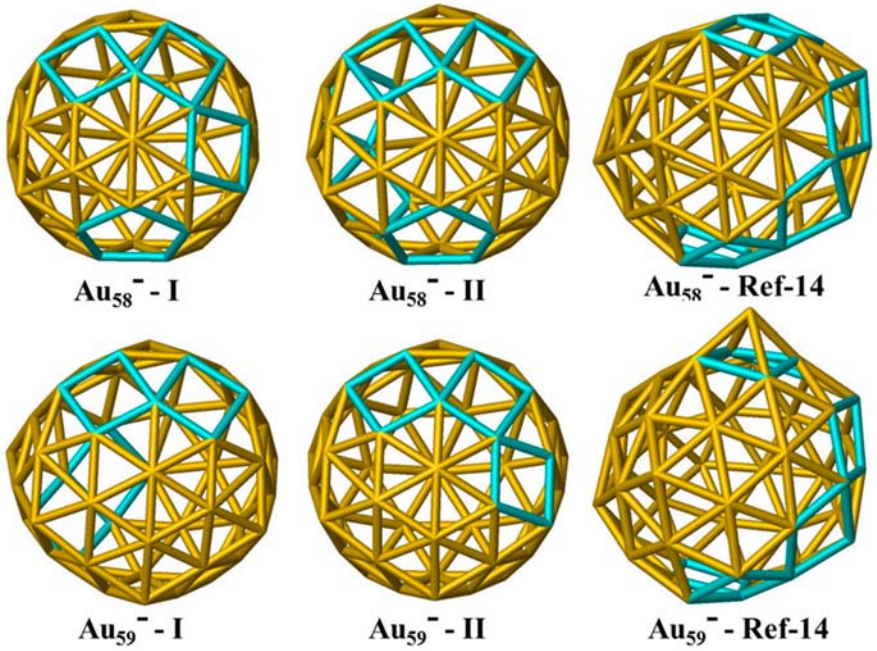

Figure 3. Structural differences among the outer shells of isomer I, isomer II, and isomers predicted in ref 14 for Au^- and Au^-. Structural (square or pentagonal) defects are highlighted in cyan color (12-atom inner core not shown).

Hence, we reoptimize all the top isomers of Au_{58}^- shown in Table S4(a) with zero charge at the PBE/DNP (ECP) level (Table S4b). Indeed, the neutral ref-14 isomer of Au_{58} exhibits higher stability than many isomers shown in Table S4a, which are more stable in anionic form.

To gain deeper understanding why the newly predicted isomers are more compact compared to those predicted in ref 14, we have analyzed the core size among top-50 and top-100 isomers collected from basin-hopping global search (**Figure S9**). One can see that for Au_{55}^-, the 9-atom core size is dominant (80%), although the newly assigned isomer exhibits a 10-atom core. For Au_{56}^-, both 9-atom (~56%) and 10-atom (~41%) core sizes are dominant, while the newly assigned major/minor isomers also exhibit 9-atom and 10-atom core sizes. For Au_{57}^-, isomers with 10-atom and 11-atom core sizes are favored, while 9-atom and 12-atom core sizes are in minority. The core of the newly assigned isomers, however, has 12 atoms. For Au_{58}^-, all top-50 isomers exhibit either 10-, 11-, or 12-atom core size while the newly assigned isomers have the 12-atom core. Lastly, for Au_{59}^-, the 12-atom core size becomes dominant, and indeed, the newly assigned isomers have the 12-atom core.

Note, however, that the rankings of these top-50 and top-100 isomers are based on the PBE level of theory. As shown in Tables S1–S5, the PBE level of theory favors isomers with relatively small core size, whereas the SO-PBE0 level of theory favors isomers with relatively large core size. In other words, consideration of the SO effect is crucial to the sensible prediction of isomers with more accurate core size. Indeed, in a previous computational study of neutral cluster Au_{58}, Dong and Gong[48] found that isomers with 10-atom core size (double shell structure) are energetically more stable than isomers with 11-atom or 12-atom core size, on the basis of the PBE level of theory without accounting for the SO effect. With accounting for the SO effect, all the four isomers with 12-atom cores reported in Table S4a show the highest stabilities compared to other isomers with 10-atom or 11-atom cores.

Au_{60}^- with a Perfect Icosahedral Core

The structures, both major and minor isomers, of Au_{60}^- exhibit many more features resembling an icosahedron like Ag_{55}^-, even though Au_{60}^- has five more atoms. Most notably, both isomers have a 13-atom icosahedral core, just like a perfect 55-atom icosahedron (**Figure 4**). Furthermore, the outer shell of isomer I exhibits C_{2v} symmetry. Both isomers exhibit two opposing 16-atom pentagonal caps in staggered confirmation, just like a perfect icosahedron. Because of the additional five atoms on the outer shell, the 10-atom single ring in the perfect icosahedron is replaced by a 6-atom single chain connected with a 9-atom double chain. Despite minor surface dissimilarities, isomer II of Au_{60}^- also exhibits nearly the same structural features as the isomer I. The close structural similarity in both isomers may be seen as the

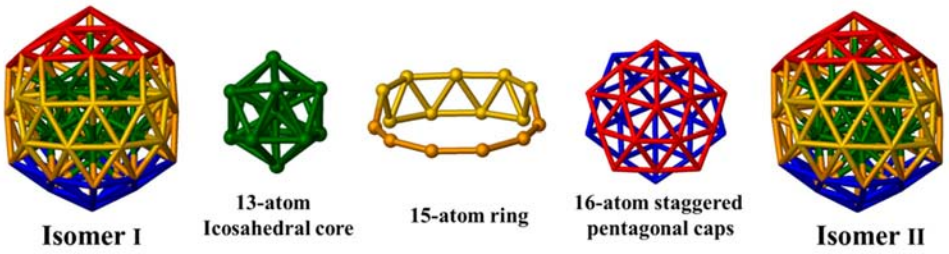

Figure 4. Two lowest-lying isomers (isomer I and isomer II) of Au^-. Both isomers exhibit an icosahedral core and an outer shell consisting of two 16-atom pentagonal caps (red and blue), a 6-atom single chain (gold), and a 9-atom double chain (yellow).

fluxional behavior of gold clusters. Overall, Au_{60}^- is the smallest core−shell gold cluster that exhibits an icosahedral core. The appearance of the icosahedral core at size n = 60 rather than the size n = 55 reflects a compromise between the trend toward icosahedron symmetry for core compactness and the strong relativistic bonding effects of gold.

Relative Stability of Gold Clusters

As pointed out by Martin, an icosahedron is a highly strained structure because the interatomic distances between shells is smaller than those within a shell, resulting in icosahedral packing energetically favorable only in relatively small-sized clusters with high surface-to-volume ratio.[49] Also, Au_{55}^- is not an icosahedral structure due largely to the relativistic effect that contracts the surface, resulting in surface holes in the outer layer.[14] The important factors such as the relativistic effects in gold and the hybridization of 5d−6s orbital effect render the prediction of the size-dependent stability of gold clusters rather complicated. [50] To compare the relative stability of the assigned major isomers, we compute the binding energy per atom, fragmentation energy, and the second-order difference in binding energy. In Figure 5 we plot these quantities versus the size n of Au_n^-, calculated at the SO-PBE0/dhf-SV(P)(ECP) level of theory. The binding energy per atom is calculated by using the equation below, where E is the energy of the gold atom, ion, or cluster:

$$E_b(Au_n^-) = \frac{(n-1)E[Au] + E[Au^-] - E[Au_n^-]}{n}$$

If the binding energy increases as n increases, the clusters would become progressively stable due to the greater delocalization of electrons. However, in **Figure 5**, Au_{57}^- gives a binding energy per atom higher than its nearest-neighboring clusters, implying higher stability than its neighbors. The fragmentation energy (ΔE_1) is calculated on the basis of the formula $\Delta E_1(Au_n^-) = E[Au_{n-1}^-] + E[Au] - E[Au_n^-]$. The plot of fragmentation energy shows an even−odd pattern, suggesting that the odd-sized Au_{57}^- and Au_{59}^- are more stable than even-sized gold clusters.

Lastly, to further analyze the relative stability, the second-order difference in binding energy, $\Delta E_2(Au_n^-) = E[Au_{n+1}^-] + E[Au_{n-1}^-] - 2E[Au_n^-]$ is computed. The second-order difference in binding energy also shows

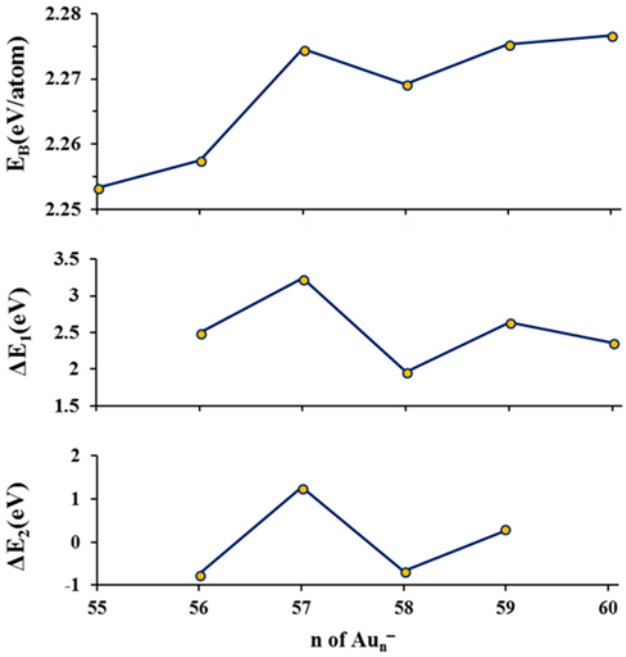

Figure 5. Computed binding energy per atom E, fragmentation energy (ΔE) and the second-order difference in binding energy (ΔE) versus the size n of Au_n^-.

even−odd oscillation behavior, suggesting that the odd-numbered clusters, Au_{57}^- and Au_{59}^-, are relatively more stable than their neighboring even-numbered clusters. Note that Au_{57}^- is an electronic "magic number" due to electronic shell closing.

In conclusion, we have found an intriguing structural evolution in midsized core−shell gold clusters; that is, both isomers of Au_{60}^- exhibit an icosahedral core. In other words, Au_{60}^- is the smallest gold cluster to accommodate an inner core of 13-atom like in a 55-atom Mackay icosahedron. The outer shell of 47 atoms exhibit two opposing 16-atom pentagonal caps. Compared to the 55-atom icosahedron, the extra 5 atoms form a chain and distort the icosahedral outer shell. Although Au_{55}^- is not a Mackay icosahedron, the structural evolution of Au_n^- (n = 55−60) shows the trend to accommodate the icosahedral core. Specifically, Au_n^- (n = 57−59) entail an inner core of 12-atoms forming an icosahedron missing an apex atom. The outer shells of Au_n^- (n = 58, 59) exhibit fragments of icosahedral caps, and the middle sections resemble the distorted pentagonal antiprism structure. Overall, the appearance of the icosahedral core at a size of n = 60 rather than the size of n = 55 reflects a compromise between the

trend toward the icosahedral core for structural compactness and the strong relativistic bonding effects of gold. Nevertheless, the identified structural evolution of the gold clusters will benefit future studies of the structure−catalytic−activity relationship.

Supporting Information

The Supporting Information follows the **References**. It is also available free of charge on the ACS Publications website at DOI: 10.1021/acs.jpclett.9b00446. Included are energy tables, simulated and experimental photoelectron spectra for all the top candidate isomers and isomers from ref 14 of anion clusters Au_n^- (n = 55−60), perfect icosahedron and minor structures of Au_n^- (n = 56−60), atom distribution from the center of mass for top candidates, bar graphs as percentage of isomers that exhibit the number of core atoms for Au_n^- (n = 55−60).

Acknowledgments — X.C.Z. thanks computation support by UNL Holland Computing Center. L.S.W. would like to thank the NSF for support of the experimental work done at Brown University. The authors declare no competing financial interest.

References

(1) Mackay, A. L. A. Dense Non-Crystallographic Packing of Equal Spheres. *Acta Crystallogr.* 1962, *15*, 916−918.
(2) Teo, B. K.; Sloane, N. J. A. Magic Numbers in Polygonal and Polyhedral Clusters. *Inorg. Chem.* 1985, *24*, 4545−4558.
(3) Kroto, H. W.; Heath, J. R.; O'Brien, S. C.; Curl, R. F.; Smalley, R. E. C. Buckminsterfullerene. *Nature* 1985, *318*, 162−163.
(4) Piotrowski, M. J.; Piquini, P.; Da Silva, J. L. F. Density Functional Theory Investigation of 3d, 4d, and 5d 13-Atom Metal Clusters. *Phys. Rev. B: Condens. Matter Mater. Phys.* 2010, *81*, 155446.
(5) Oviedo, J.; Palmer, R. E. Amorphous Structures of Cu, Ag, and Au Nanoclusters from First Principles Calculations. *J. Chem. Phys.* 2002, *117*, 9548−9551.
(6) Chang, C. M.; Chou, M. Y. Alternative Low-Symmetry Structure for 13-Atom Metal Clusters. *Phys. Rev. Lett.* 2004, *93*, 133401.
(7) Häkkinen, H.; Yoon, B.; Landman, U.; Li, X.; Zhai, H.-J.; Wang, L.-S. On the Electronic and Atomic Structures of Small Au_n^- (n = 4−14) Clusters: A Photoelectron Spectroscopy and Density-Functional Study. *J. Phys. Chem. A* 2003, *107*, 6168−6175.

(8) Häkkinen, H.; Moseler, M. 55-Atom Clusters of Silver and Gold: Symmetry Breaking by Relativistic Effects. *Comput. Mater. Sci.* 2006, *35*, 332−336.
(9) Rapps, T.; Ahlrichs, R.; Waldt, E.; Kappes, M. M.; Schooss, D. On the Structures of 55-Atom Transition-Metal Clusters and Their Relationship to the Crystalline Bulk. *Angew. Chem., Int. Ed.* 2013, *52*, 6102−6105.
(10) Xing, X.; Danell, R. M.; Garzón, I. L.; Michaelian, K.; Blom, M. N.; Burns, M. M.; Parks, J. H. Size-Dependent Fivefold and Icosahedral Symmetry in Silver Clusters. *Phys. Rev. B: Condens. Matter Mater. Phys.* 2005, *72*, 081405.
(11) Schooss, D.; Blom, M. N.; Parks, J. H.; Issendorff, B. V.; Haberland, H.; Kappes, M. M. The Structures of Ag_{55}^{+} and Ag_{55}^{-}: Trapped Ion Electron Diffraction and Density Functional Theory. *Nano Lett.* 2005, *5*, 1972−1977.
(12) Häkkinen, H.; Moseler, M.; Kostko, O.; Morgner, N.; Hoffmann, M. A.; v. Issendorff, B. Symmetry and Electronic Structure of Noble-Metal Nanoparticles and the Role of Relativity. *Phys. Rev. Lett.* 2004, *93*, 093401.
(13) Garzón, I. L.; Michaelian, K.; Beltrán, M. R.; Posada-Amarillas, A.; Ordejón, P.; Artacho, E.; Sánchez-Portal, D.; Soler, J. M. Lowest Energy Structures of Gold Nanoclusters. *Phys. Rev. Lett.* 1998, *81*, 1600−1603.
(14) Huang, W.; Ji, M.; Dong, C.-D.; Gu, X.; Wang, L.-M.; Gong, X. G.; Wang, L.-S. Relativistic Effects and the Unique Low-Symmetry Structures of Gold Nanoclusters. *ACS Nano* 2008, *2*, 897−904.
(15) Haruta, M.; Tsubota, S.; Kobayashi, T.; Kageyama, H.; Genet, M. J.; Delmon, B. Low-Temperature Oxidation of CO over Gold Supported on TiO_2, α-Fe_2O_3, and Co_3O_4. *J. Catal.* 1993, *144*, 175− 192.
(16) Haruta, M.; Kobayashi, T.; Sano, H.; Yamada, N. Novel Gold Catalysts for the Oxidation of Carbon Monoxide at a Temperature Far below 0°C. *Chem. Lett.* 1987, *16*, 405−408.
(17) Lopez, N.; Janssens, T. V. W.; Clausen, B. S.; Xu, Y.; Mavrikakis, M.; Bligaard, T.; Nørskov, J. K. On the Origin of the Catalytic Activity of Gold Nanoparticles for Low-Temperature CO Oxidation. *J. Catal.* 2004, *223*, 232−235.
(18) Haruta, M. Size- and Support-Dependency in the Catalysis of Gold. *Catal. Today* 1997, *36*, 153−166.
(19) Chen, M. S.; Goodman, D. W. Structure-Activity Relationships in Supported Au Catalysts. *Catal. Today* 2006, *111*, 22−33.
(20) Li, L.; Gao, Y.; Li, H.; Zhao, Y.; Pei, Y.; Chen, Z.; Zeng, X. C. CO Oxidation on TiO_2 (110) Supported Subnanometer Gold Clusters: Size and Shape Effects. *J. Am. Chem. Soc.* 2013, *135*, 19336−19346.
(21) Häkkinen, H. Atomic and Electronic Structure of Gold Clusters: Understanding Flakes, Cages and Superatoms from Simple Concepts. *Chem. Soc. Rev.* 2008, *37*, 1847.
(22) Wang, L.-M.; Wang, L.-S. Probing the Electronic Properties and Structural Evolution of Anionic Gold Clusters in the Gas Phase. *Nanoscale* 2012, *4*, 4038.
(23) Li, J.; Li, X.; Zhai, H.-J.; Wang, L.-S. Au : A Tetrahedral Cluster. *Science* 2003, *299*, 864−867.
(24) Knight, W. D.; Clemenger, K.; De Heer, W. A.; Saunders, W. A.; Chou, M. Y.; Cohen, M. L. Electronic Shell Structure and Abundances of Sodium Clusters. *Phys. Rev. Lett.* 1984, *52*, 2141− 2143.

(25) Shao, N.; Huang, W.; Gao, Y.; Wang, L.-M.; Li, X.; Wang, L.-S.; Zeng, X. C. Probing the Structural Evolution of Medium-Sized Gold Clusters: Au_n^- (n = 27−35). *J. Am. Chem. Soc.* 2010, *132*, 6596− 6605.
(26) Shao, N.; Huang, W.; Mei, W.-N.; Wang, L. S.; Wu, Q.; Zeng, X. C. Structural Evolution of Medium-Sized Gold Clusters Au^- (n = 36, 37, 38): Appearance of Bulk-Like Face Centered Cubic Fragment. *J. Phys. Chem. C* 2014, *118*, 6887−6892.
(27) Pande, S.; Huang, W.; Shao, N.; Wang, L. M.; Khetrapal, N.; Mei, W. N.; Jian, T.; Wang, L. S.; Zeng, X. C. Structural Evolution of Core-Shell Gold Nanoclusters: Au_n^- (n = 42−50). *ACS Nano* 2016, *10*, 10013−10022. (28) Heiles, S.; Johnston, R. L. Global Optimization of Clusters Using Electronic Structure Methods. *Int. J. Quantum Chem.* 2013, *113*, 2091.
(29) Wales, D. J.; Doye, J. P. K. Global Optimization by Basin- Hopping and the Lowest Energy Structures of Lennard-Jones Clusters Containing up to 110 Atoms. *J. Phys. Chem. A* 1997, *101*, 5111−5116.
(30) Wales, D. J.; Scheraga, H. a. Global Optimization of Clusters, Crystals, and Biomolecules. *Science* 1999, *285*, 1368−1372.
(31) Pande, S.; Jian, T.; Khetrapal, N. S.; Wang, L.-S.; Zeng, X. C. Structural Evolution of Gold-Doped Bismuth Clusters $AuBi_n^-$ (n = 4−8). *J. Phys. Chem. C* 2018, *122*, 6947−6954.
(32) Khetrapal, N. S.; Jian, T.; Pal, R.; Lopez, G. V.; Pande, S.; Wang, L.-S.; Zeng, X. C. Probing the Structures of Gold−aluminum Alloy Clusters $Au_xAl_y^-$: A Joint Experimental and Theoretical Study. *Nanoscale* 2016, *8*, 9805−9814.
(33) Khetrapal, N. S.; Jian, T.; Lopez, G. V.; Wang, L.-S.; Zeng, X. C. Probing the Structural Evolution of Gold−Aluminum Bimetallic Clusters ($Au_2Al_n^-$, n = 3−11) Using Photoelectron Spectroscopy and Theoretical Calculations. *J. Phys. Chem. C* 2017, *121*, 18234.
(34) Pal, R.; Wang, L.-M.; Huang, W.; Wang, L.-S.; Zeng, X. C. Structure Evolution of Gold Cluster Anions between the Planar and Cage Structures by Isoelectronic Substitution: Au_n^- (n = 13−15) and $M Au_n^-$ (n = 12−14; M = Ag, Cu). *J. Chem. Phys.* 2011, *134*, 054306.
(35) Huang, W.; Pal, R.; Wang, L.-M.; Zeng, X. C.; Wang, L.-S. Isomer Identification and Resolution in Small Gold Clusters. *J. Chem. Phys.* 2010, *132*, 054305.
(36) Wang, L. M.; Pal, R.; Huang, W.; Zeng, X. C.; Wang, L. S. Observation of Earlier Two-to-Three Dimensional Structural Transition in Gold Cluster Anions by Isoelectronic Substitution: $M Au_n^-$ (n = 8−11; M = Ag,Cu). *J. Chem. Phys.* 2010, *132*, 114306.
(37) Perdew, J.; Burke, K.; Ernzerhof, M. Generalized Gradient Approximation Made Simple. *Phys. Rev. Lett.* 1996, *77*, 3865−3868.
(38) Delley, B. An All-Electron Numerical Method for Solving the Local Density Functional for Polyatomic Molecules. *J. Chem. Phys.* 1990, *92*, 508−517.
(39) Delley, B. From Molecules to Solids with the DMol3 Approach. *J. Chem. Phys.* 2000, *113*, 7756−7764.
(40) te Velde, G.; Bickelhaupt, F. M.; Baerends, E. J.; Fonseca Guerra, C.; van Gisbergen, S. J. a.; Snijders, J. G.; Ziegler, T. Chemistry with ADF. *J. Comput. Chem.* 2001, *22*, 931−967.

(41) Fonseca Guerra, C.; Snijders, J. G.; Te Velde, G.; Baerends, E. J. Towards an Order- N DFT Method. *Theor. Chem. Acc.* 1998, *99*, 391−403.
(42) *ADF Release 2013; Software for Chemistry and Materials (SCM)*; Vrije Universiteit, Amsterdam, The Netherlands, https://www.scm.com
(43) Adamo, C.; Barone, V. Toward Reliable Density Functional Methods without Adjustable Parameters: The PBE0 Model. *J. Chem. Phys.* 1999, *110*, 6158−6170.
(44) Valiev, M.; Bylaska, E. J.; Govind, N.; Kowalski, K.; Straatsma, T. P.; Van Dam, H. J. J.; Wang, D.; Nieplocha, J.; Apra, E.; Windus, T. L.; et al. NWChem: A Comprehensive and Scalable Open-Source Solution for Large Scale Molecular Simulations. *Comput. Phys. Commun.* 2010, *181*, 1477−1489.
(45) Ross, R. B.; Powers, J. M.; Atashroo, T.; Ermler, W. C.; LaJohn, L. A.; Christiansen, P. A. Ab Initio Relativistic Effective Potentials with Spin−orbit Operators. IV. Cs through Rn. *J. Chem. Phys.* 1990, *93*, 6654.
(46) Weigend, F.; Baldes, A. Segmented Contracted Basis Sets for One- and Two-Component Dirac−Fock Effective Core Potentials. *J. Chem. Phys.* 2010, *133*, 174102.
(47) Mantina, M.; Valero, R.; Truhlar, D. G. Validation Study of the Ability of Density Functionals to Predict the Planar-to-Three- Dimensional Structural Transition in Anionic Gold Clusters. *J. Chem. Phys.* 2009, *131*, 064706.
(48) Dong, C. D.; Gong, X. G. Gold Cluster beyond Hollow Cage: A Double Shell Structure of Au . *J. Chem. Phys.* 2010, *132*, 104301.
(49) Martin, T. P. Shells of Atoms. *Phys. Rep.* 1996, *273*, 199−241.
(50) Pyykko, E. Relativistic Effects in Structural Chemistry. *Chem. Rev.* 1988, *88*, 563−594.

Supporting Information

Au_{60}^-: The Smallest Gold Cluster with the High-Symmetry Icosahedral Core Au_{13}

Seema Pande[1], Xingao Gong[2], Lai-Sheng Wang[3]*, Xiao Cheng Zeng[1]*

[1]Department of Chemistry, University of Nebraska-Lincoln, Lincoln, Nebraska 68588

[2]Department of Physics, Fudan University, Shanghai, 200433, China

[3]Department of Chemistry, Brown University, Providence, RI 02912

*E-mails: xzeng1@unl.edu; Lai-Sheng_Wang@Brown.edu

Specification for the tables presented below: Isomer Number is the ranking based on energy calculations at the PBE/DND(ECP) (fine) level for the respective clusters. Relative energies: ΔE^a at PBE/DNP(ECP) (fine Integration grid), ΔE^b at PBE0/TZP(ECP), ΔE^c at SO-PBE0/CRENBL(ECP) (for Au_n^-, n=55-58) and SO-PBE0/dhf-SV(P)(ECP) (for Au_n^-, n=59-60 level of theory, RMSD is the root mean square deviation of the simulated peaks when the simulated first VDE is aligned with the experimental first VDE (units of values in columns 3-8 is eV). Highlighted in red in all Supporting Tables are the isomers whose figures are presented in the main text, with final ranking in roman number based on the best overall agreement with the experimental photoelectron spectra.

"Ref-14" are the isomers previously published in reference 14 of the main text.

Table S1: Electronic properties of cluster Au_{55}^-. The unit is eV for column 3 – 8.

Isomer No. Au_{55}-	**No. of core atom**	**ΔE^a**	**ΔE^b**	**ΔE^c**	**VDE**	**Energy gap[c]**	**RMSD**
2	9	0.000	0.000	0.100	4.16	0.10	0.0494
3	9	0.005	0.161	0.279	4.16	0.05	0.0784
5	9	0.011	0.127	0.332	4.20	0.09	0.1032
6	9	0.011	0.168	0.316	4.16	0.07	0.0775
7	9	0.013	0.129	0.294	4.18	0.13	0.0546
9	9	0.030	0.082	0.193	4.12	0.11	0.0626
10	10	0.041	0.165	0.038	4.08	0.12	0.0493
11(I)	**10**	**0.045**	**0.148**	**0**	**4.12**	**0.10**	**0.0493**
12	9	0.048	0.064	0.196	4.18	0.07	0.099
13	9	0.051	0.072	0.232	4.11	0.11	0.0708
16	10	0.072	0.254	0.077	4.07	0.11	0.0572
Ref-14	10	0.256	0.444	0.341	4.08	0.13	0.0579

Table S2: Electronic properties of cluster Au_{56}^-. The unit is eV for column 3 – 8.

Isomer No. Au_{56}^-	No. of core atom	ΔE^a	ΔE^b	ΔE^c	VDE	Energy gap [c]	RMSD
1 (II)	**9**	**0.000**	**0.000**	**0.078**	**3.89**	**0.29**	**0.0700**
3	9	0.060	0.080	0.160	3.90	0.29	0.0872
7	10	0.076	0.203	0.032	3.95	0.20	2.0717
11 (I)	**10**	**0.090**	**0.255**	**0**	**3.91**	**0.21**	**0.0297**
23	9	0.148	0.179	0.196	3.85	0.35	0.3645
25	9	0.149	0.172	0.269	3.9	0.30	0.2239
35	10	0.165	0.284	0.171	3.94	0.25	0.2947
39	10	0.170	0.272	0.108	3.93	0.24	0.0324
42	10	0.183	0.255	0.141	3.92	0.29	0.4337
49	10	0.193	0.262	0.099	3.92	0.29	0.0441
Ref-14	11	0.353	0.637	0.140	4.07	0.10	0.1928

Table S3: Electronic properties of cluster Au_{57}^-. The unit is eV for column 3 – 8.

Isomer No. Au_{57}^-	No. of core atom	ΔE^a	ΔE^b	ΔE^c	VDE	Energy gap [c]	RMSD
5	10	0.000	0.054	0.400	4.22	0.02	**0.1875**
10	9	0.053	0.000	0.636	4.14	0.09	**0.1057**
15	9	0.082	0.058	0.593	4.22	0.10	0.0839
26	9	0.135	0.132	0.716	4.21	0.13	0.1379
33	11	0.157	0.298	0.330	4.19	0.07	0.1723
34(II)	**12**	**0.160**	**0.374**	**0.000**	**4.20**	**0.13**	**0.1056**
35(I)	**12**	**0.171**	**0.425**	**0.014**	**4.17**	**0.09**	**0.0692**
43	12	0.197	0.401	0.112	4.17	0.06	0.2076
56	12	0.212	0.433	0.145	4.20	0.03	0.2211
Ref-14	11	0.215	0.373	0.319	4.07	0.13	0.1069

Table S4a: Electronic properties of cluster Au_{58}^-. The unit is eV for column 3 – 8.

Isomer No. Au_{58}^-	No. of core atom	ΔE^a	ΔE^b	ΔE^c	VDE	Energy gap[c]	RMSD
1	10	0.000	0.000	0.234	3.71	0.45	0.1037
14	10	0.106	0.088	0.432	3.65	0.65	0.1051
15	11	0.109	0.238	0.071	3.66	0.63	0.1811
23 (I)	**12**	**0.153**	**0.363**	**0.000**	**3.61**	**0.58**	**0.0776**
26 (II)	**12**	**0.165**	**0.375**	**0.022**	**3.62**	**0.61**	**0.0736**
28	12	0.170	0.320	0.002	3.65	0.58	0.1085
45	11	0.238	0.426	0.228	3.61	0.65	0.0679
62	11	0.268	0.447	0.456	3.60	0.59	0.0259
70	11	0.288	0.447	0.485	3.61	0.68	0.0401
87	11	0.307	0.426	0.424	3.62	0.60	0.0760
88	11	0.308	0.510	0.498	3.61	0.53	0.0677
101	11	0.325	0.389	0.455	3.74	0.46	0.1827
116	11	0.342	0.502	0.472	3.67	0.61	0.1882
131	11	0.353	0.486	0.561	3.62	0.63	0.0622
Ref-14	12	0.331	0.608	0.212	3.48	0.75	0.0688

Table S4b: Relative energy of isomers optimized with neutral charge at PBE/DNP(ECP) level

Isomer No. Au_{58}	ΔE
1	0.000
14	0.081
15	0.083
23 (I)	**0.094**
26 (II)	**0.123**
28	0.132
45	0.189
62	0.231
70	0.252
87	0.261
88	0.257
101	0.298
116	0.296
131	0.316
Ref-14	0.212

Table S5: Electronic properties of cluster Au_{59}^-. The unit is eV for column 3 – 8.

Isomer No. Au_{59}^-	No. of core atom	ΔE^a	ΔE^b	ΔE^c	VDE	Energy gap[c]	RMSD
1(II)	**12**	**0**	**0.059**	**0.041**	**3.57**	**0.68**	**0.0808**
7(I)	**12**	**0.051**	**0**	**0**	**3.63**	**0.63**	**0.0258**
8	12	0.173	0.197	0.131	3.57	0.69	0.0983
11	12	0.203	0.268	0.229	3.52	0.78	0.1562
14	11	0.255	0.153	0.856	3.64	0.65	0.1119
16	11	0.263	0.319	0.924	3.58	0.68	0.1241
18	12	0.277	0.309	0.262	3.56	0.72	0.0979
19	12	0.284	0.245	0.295	3.60	0.71	0.1239
23	11	0.309	0.298	0.935	3.56	0.76	0.1663
24	12	0.309	0.334	0.611	3.56	0.79	0.1757
Ref-14	12	0.522	0.610	0.574	3.52	0.77	0.1576

Table S6: Electronic properties of cluster Au_{59}^-. The unit is eV for column 3 – 8.

Isomer No. Au_{60}^-	No. of core atom	ΔE^a	ΔE^b	ΔE^c	VDE	Energy gap[c]	RMSD
2	11	0	0	0.610	3.74	0.23	0.2543
3 (I)	**13**	**0.055**	**0.334**	**0**	**3.36**	**0.19**	**0.0885**
5	12	0.104	0.218	0.288	3.56	0.21	0.1419
6 (II)	**13**	**0.126**	**0.381**	**0.052**	**3.37**	**0.21**	**0.1196**
14	11	0.196	0.285	1.074	3.65	0.22	0.1969
15	12	0.209	0.336	0.386	3.54	0.21	0.1208
22	12	0.239	0.193	0.201	3.53	0.40	0.1415
25	10	0.249	0.317	0.950	3.59	0.26	0.1254
28	12	0.258	0.411	0.695	3.55	0.18	0.0975
33	12	0.261	0.306	0.397	3.53	0.25	0.2092
37	11	0.265	0.374	1.121	3.54	0.22	0.0923
43	12	0.275	0.424	0.697	3.47	0.28	0.0892
44	11	0.281	0.345	0.965	3.60	0.22	0.1877
52	11	0.298	0.318	0.909	3.71	0.19	0.2030
Ref-14	12	0.202	0.505	0.752	3.48	0.22	0.0861

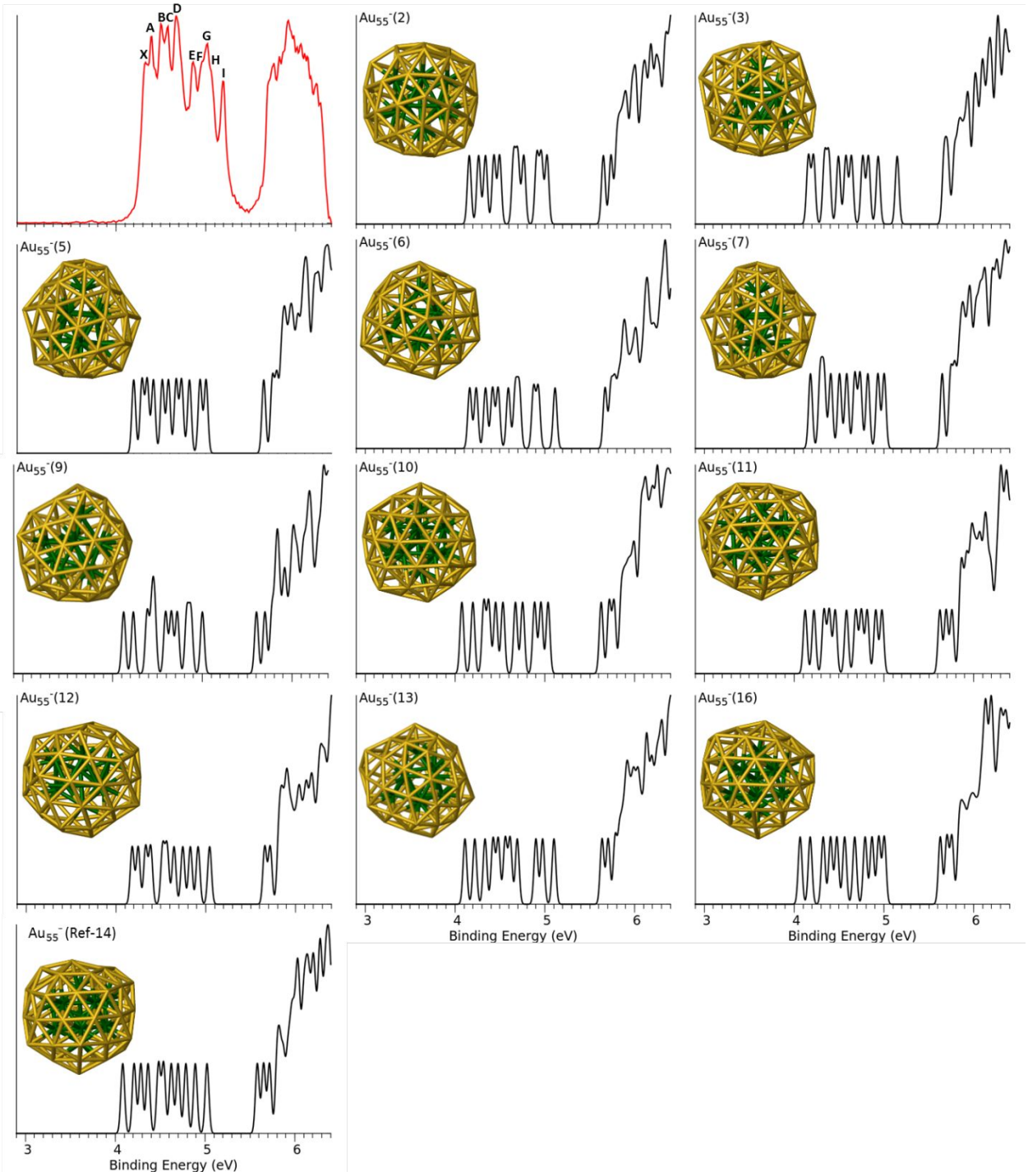

Figure S1: Experimental PES spectrum and simulated spectra of all top candidates of Au_{55}^-.

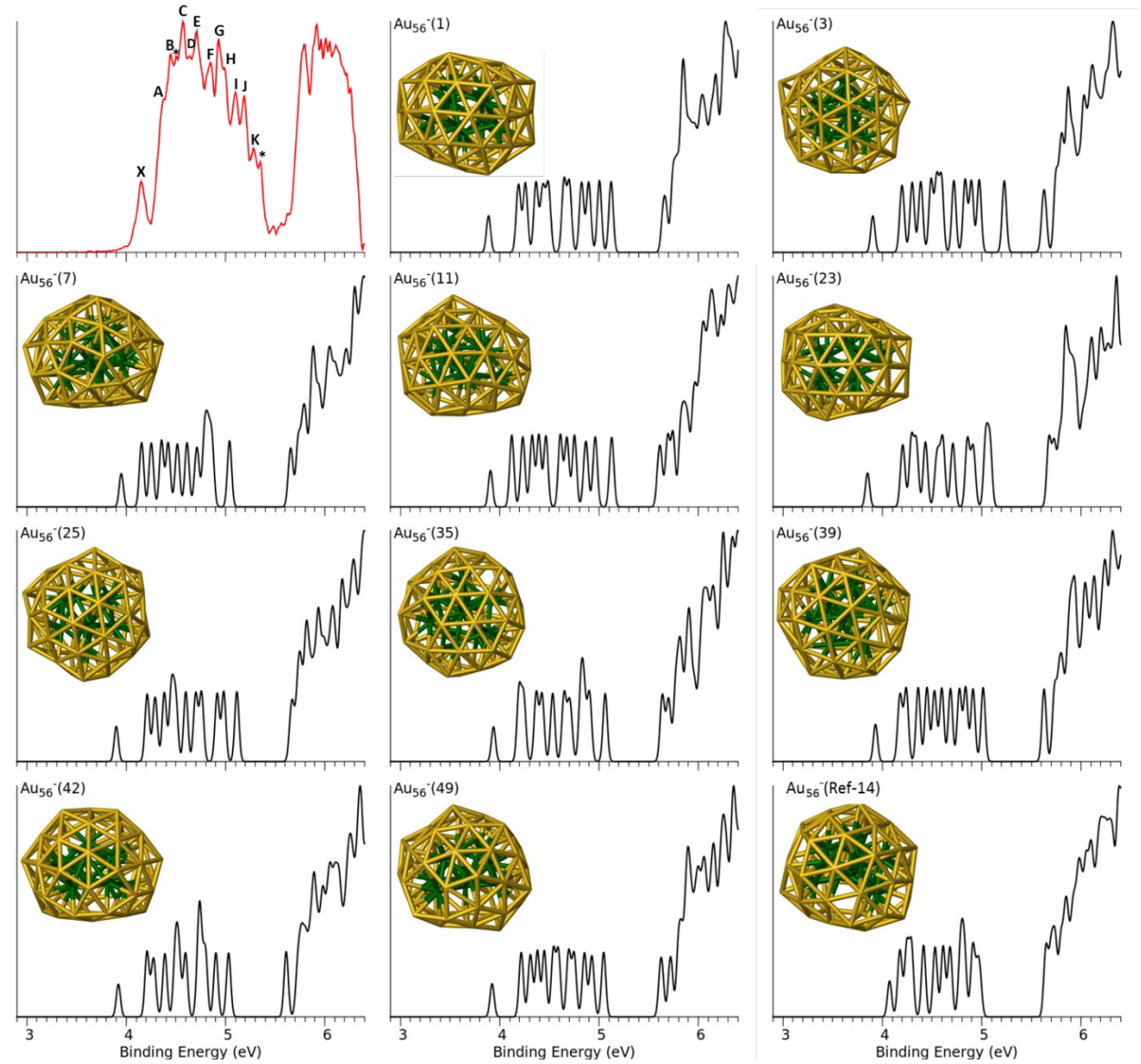

Figure S2: Experimental PES spectrum and simulated spectra of all top candidates of Au_{56}^-.

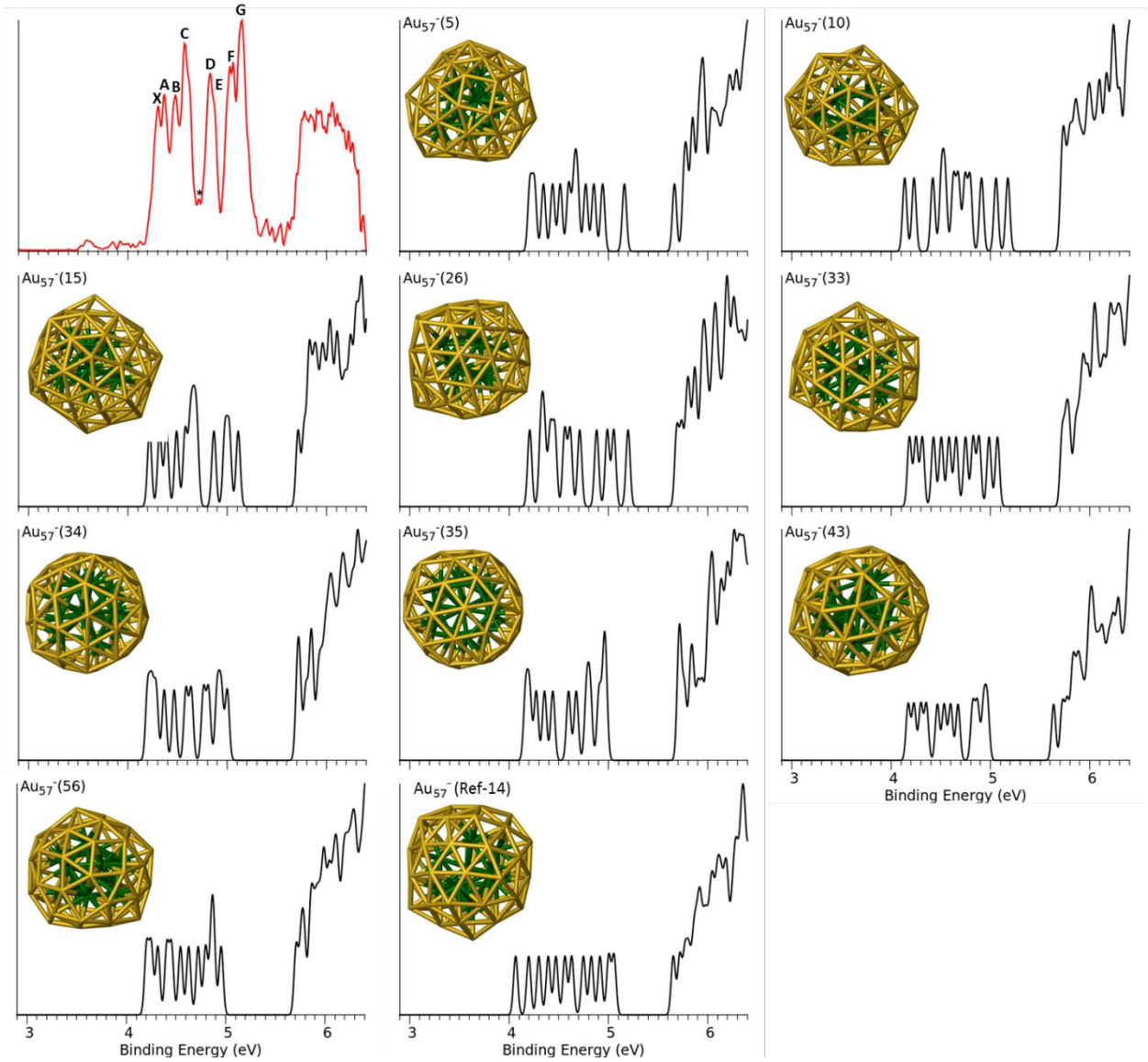

Figure S3: Experimental PES spectrum and simulated spectra of all top candidates of Au_{57}^-.

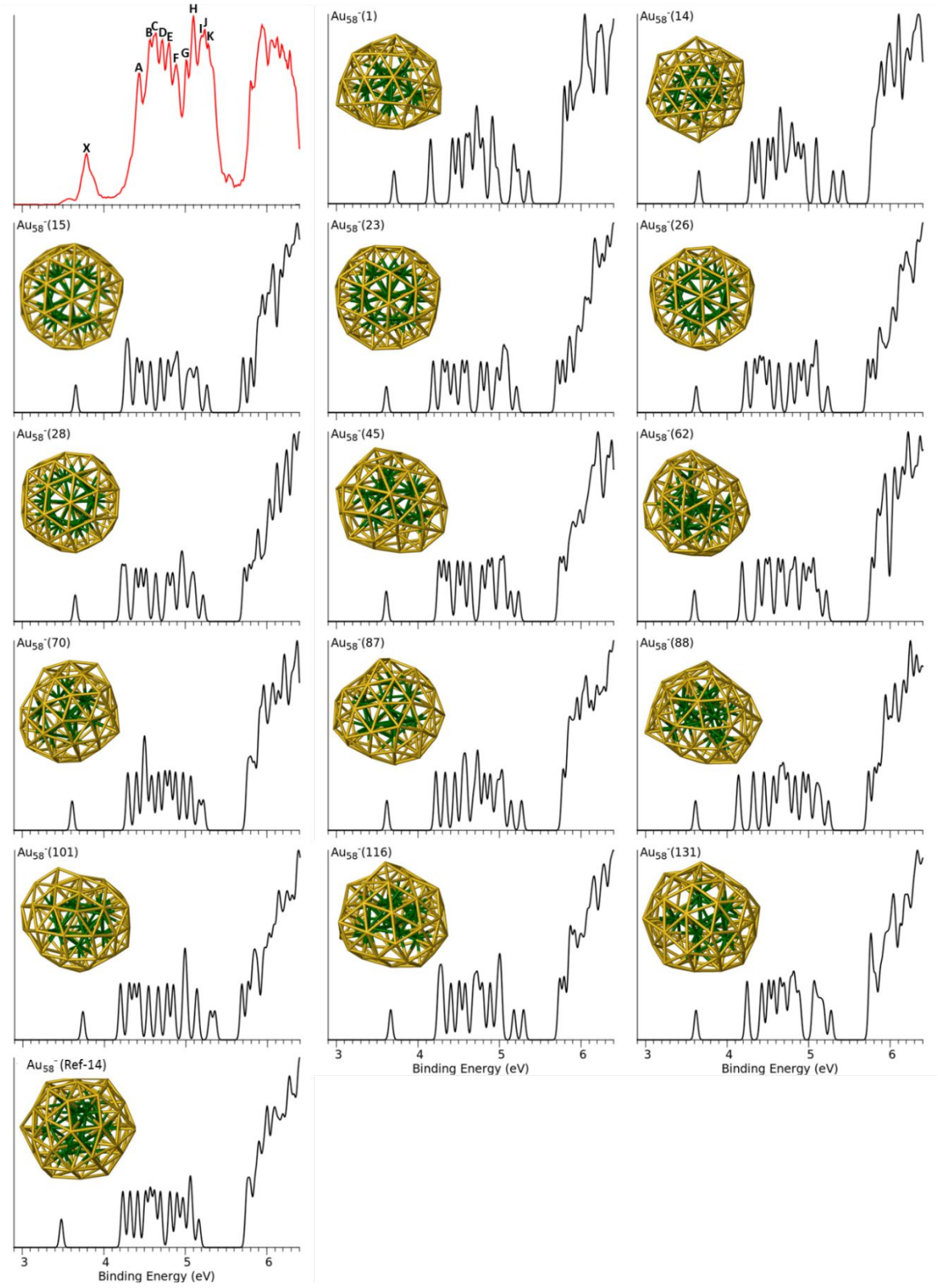

Figure S4: Experimental PES spectrum and simulated spectra of all top candidates of Au_{58}^-.

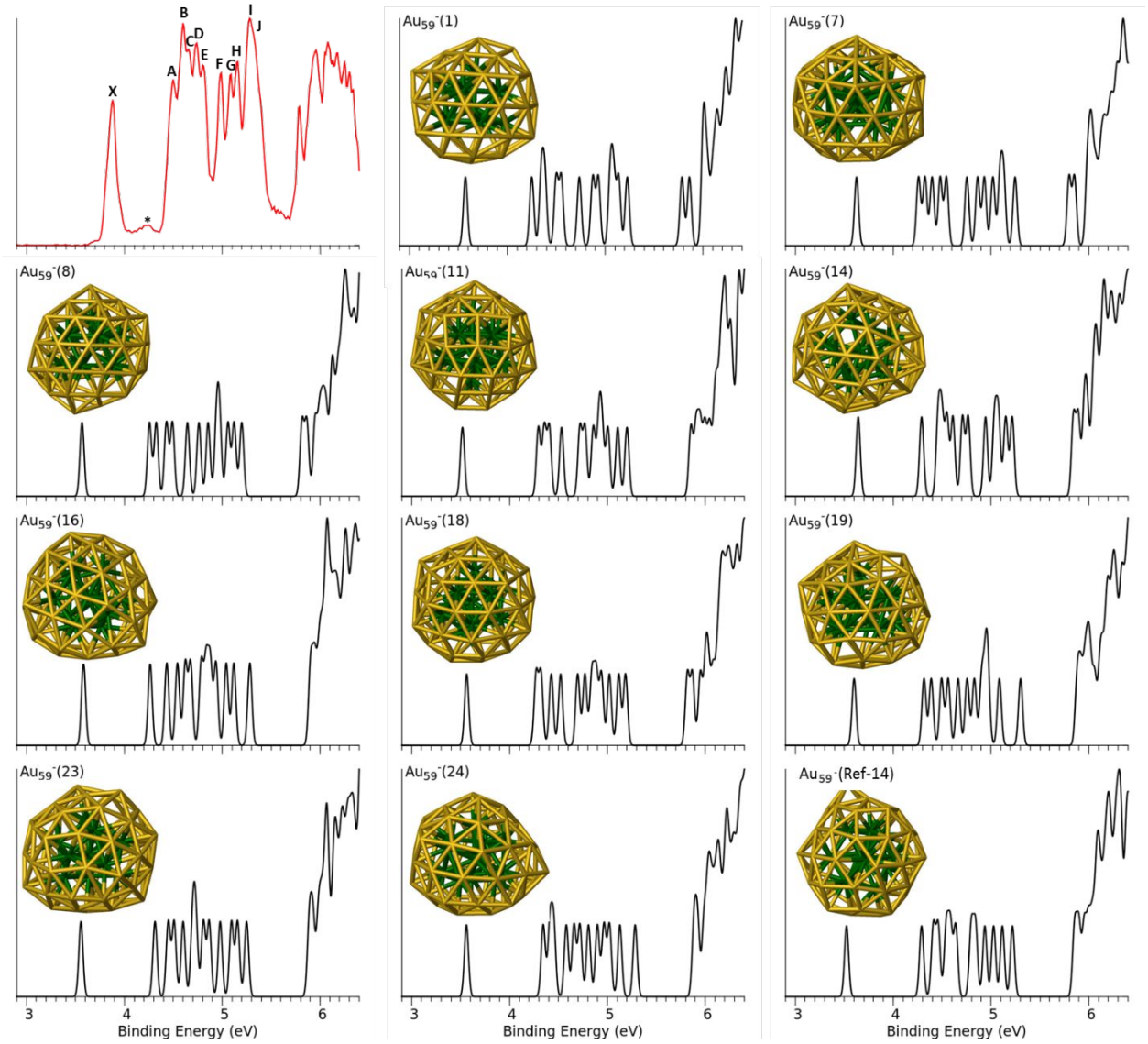

Figure S5: Experimental PES spectrum and simulated spectra of all top candidates of Au_{59}^-.

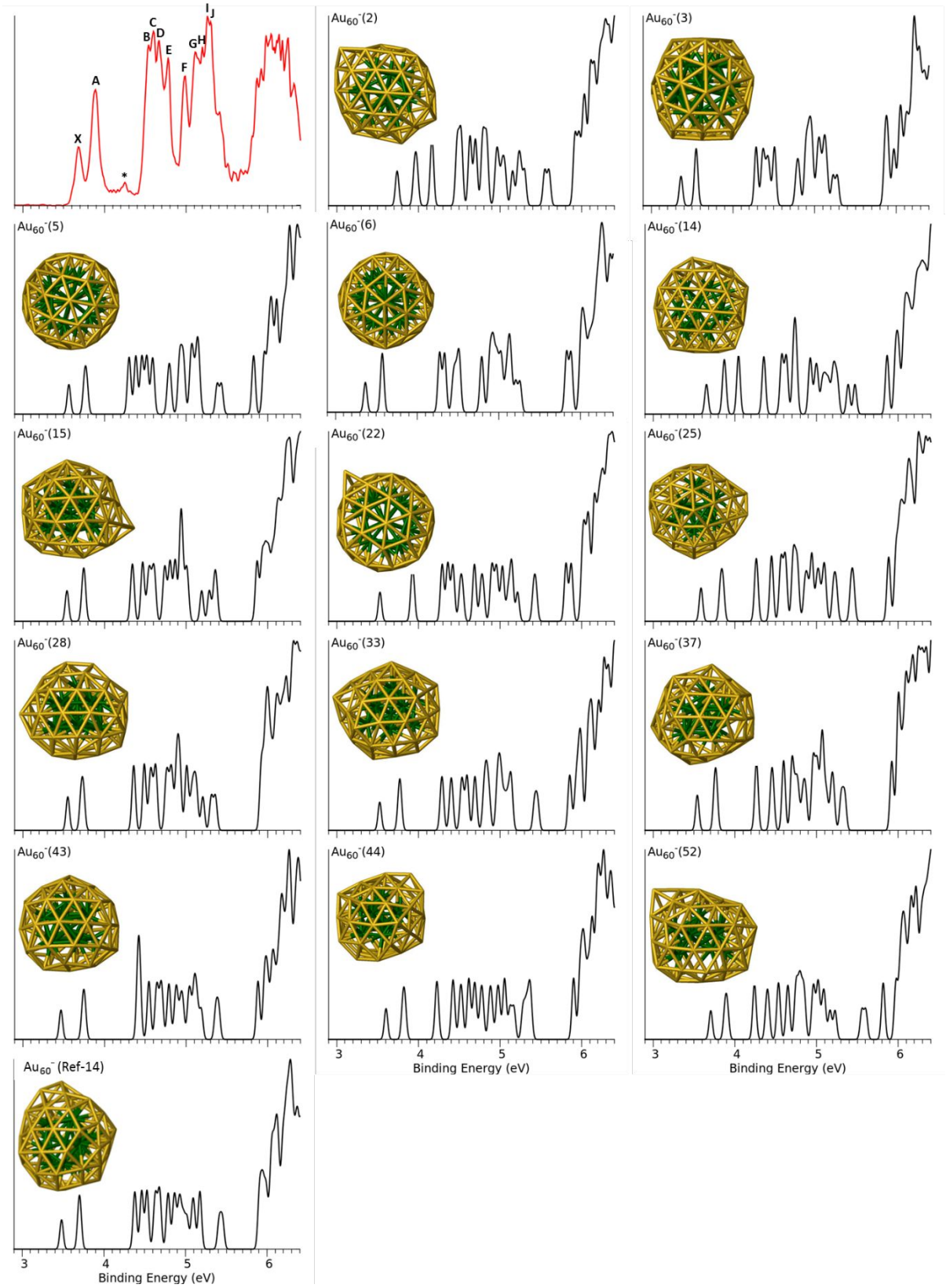

Figure S6: Experimental PES spectrum and simulated spectra of all top candidates of Au_{60}^-.

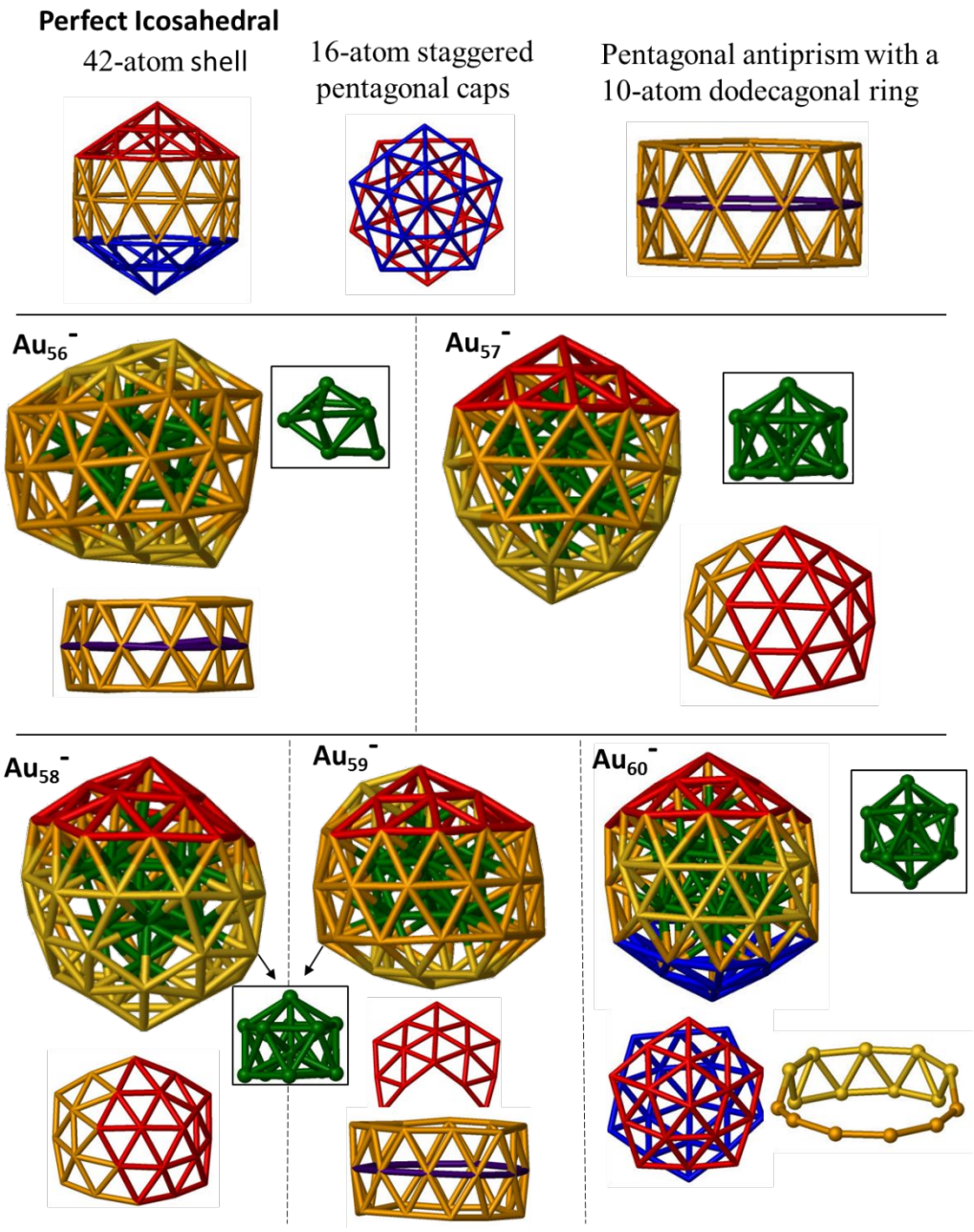

Figure S7: Top panel: a perfect icosahedron shell of 42 atoms with two pentagonal caps (red and blue) and a pentagon anti-prism with a 10-atom dodecagonal ring (purple). Middle and bottom panels: The same color coding is used to compare the assigned minor structures of Au_n^- (n = 56-60): Red and blue highlight fragments of pentagon cap, while the purple color highlights the 11-atom ring. Insets in green display the core. For Au_{60}^- 6-atom single chain (gold) and a 9-atom double chain (yellow).

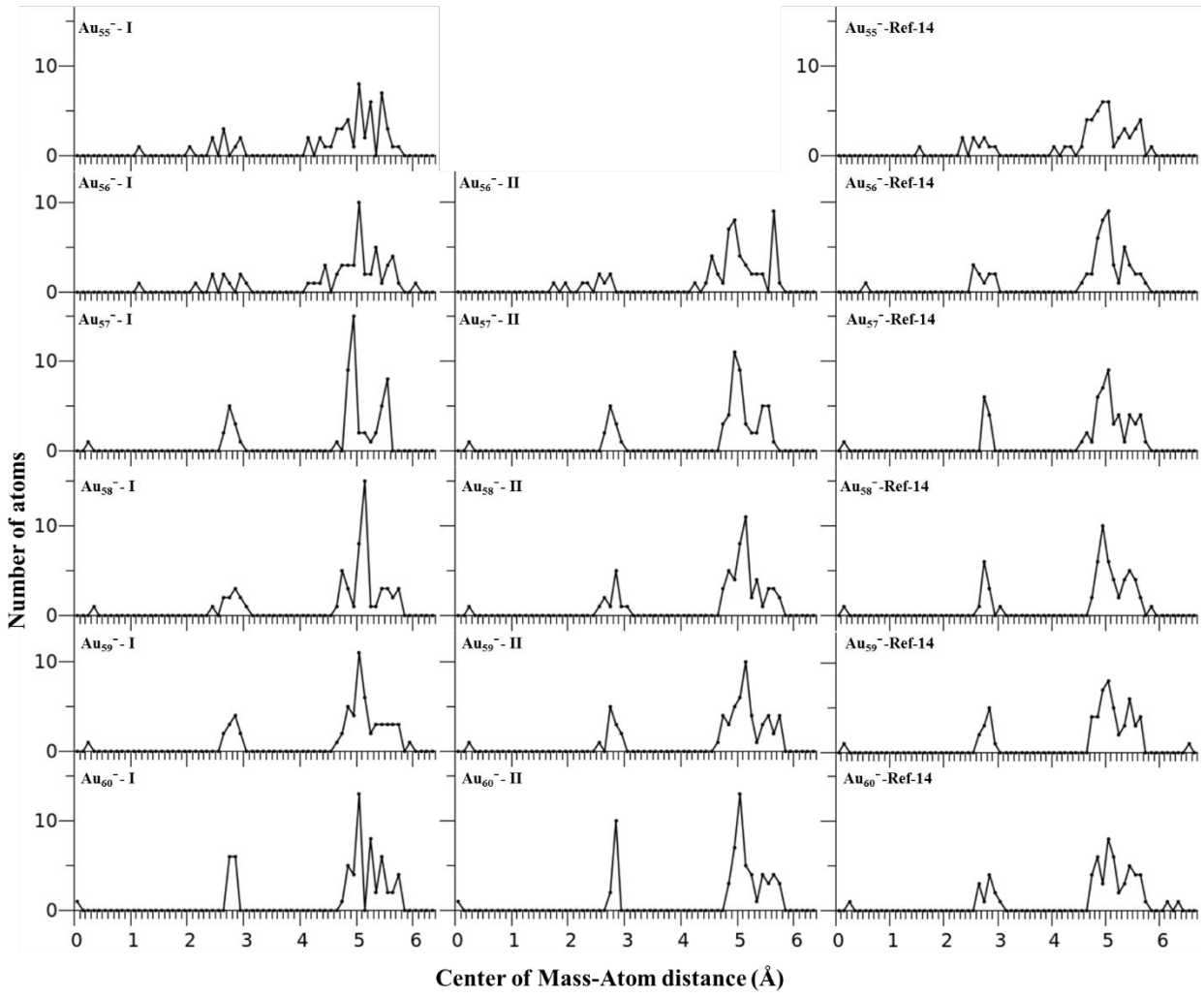

Figure S8: The relative distribution of atoms from the center of mass for top isomers presented in main text and isomers from reference14**.**

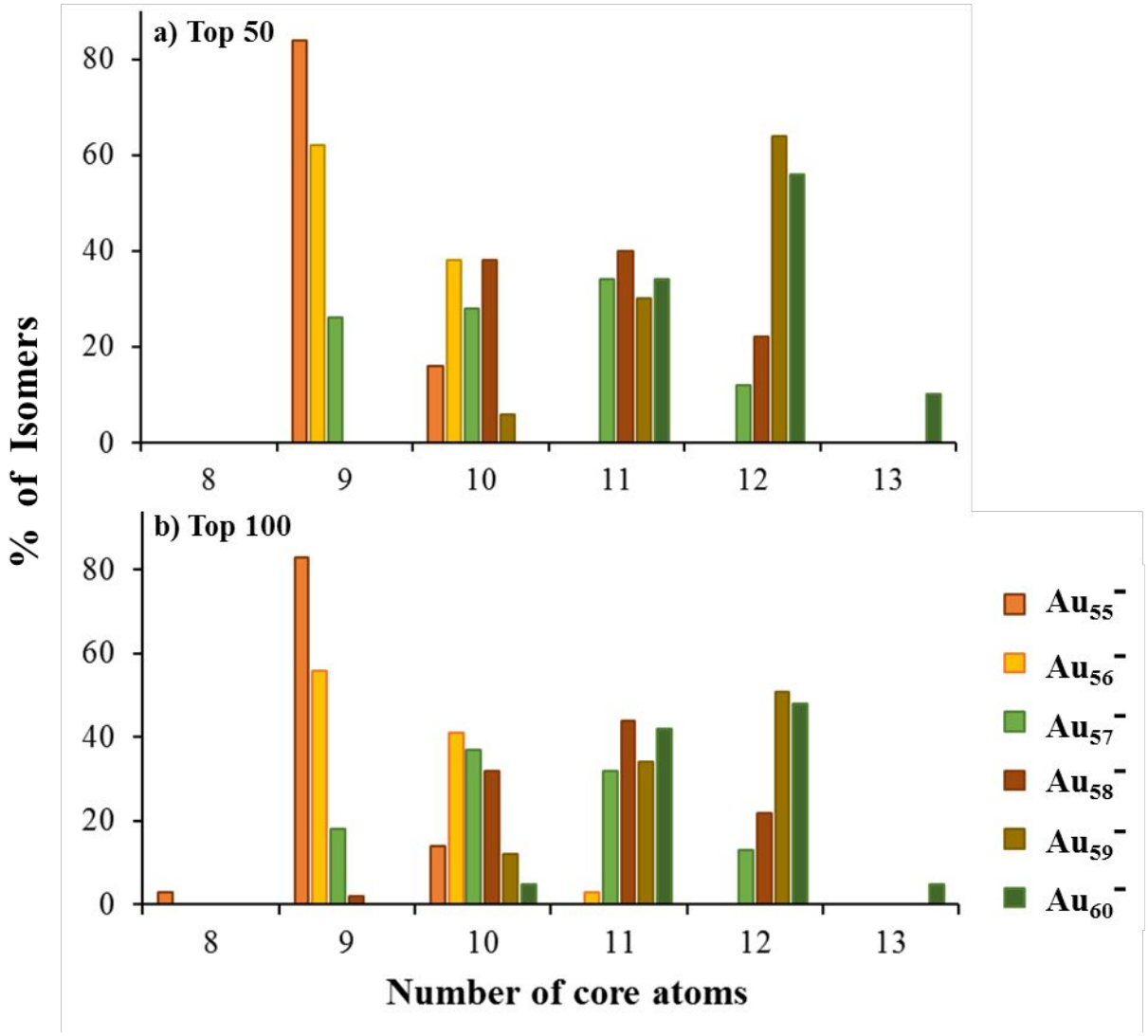

Figure S9: The bar graph represents the corresponding percentage of Isomers that exhibit the number of core atoms in x axis, for the size range Au_n^- (n=55-60). a) presents the distribution in top 50 isomers b) presents the distribution in top 100 isomers.